

Closing the loop between neural network simulators and the OpenAI Gym

Jakob Jordan^{1,2,3*†}Philipp Weidel^{2,1,3*}Abigail Morrison^{2,1,3}¹ Institute of Neuroscience and Medicine (INM-6), Research Centre Jülich, Jülich, Germany² Institute for Advanced Simulation (IAS-6), Research Centre Jülich, Jülich, Germany³ JARA-Institute Brain Structure Function Relationship (JBI 1 / INM-10), Research Centre Jülich, Jülich, Germany

Abstract

Since the enormous breakthroughs in machine learning over the last decade, functional neural network models are of growing interest for many researchers in the field of computational neuroscience. One major branch of research is concerned with biologically plausible implementations of reinforcement learning, with a variety of different models developed over the recent years. However, most studies in this area are conducted with custom simulation scripts and manually implemented tasks. This makes it hard for other researchers to reproduce and build upon previous work and nearly impossible to compare the performance of different learning architectures. In this work, we present a novel approach to solve this problem, connecting benchmark tools from the field of machine learning and state-of-the-art neural network simulators from computational neuroscience. This toolchain enables researchers in both fields to make use of well-tested high-performance simulation software supporting biologically plausible neuron, synapse and network models and allows them to evaluate and compare their approach on the basis of standardized environments of varying complexity. We demonstrate the functionality of the toolchain by implementing a neuronal actor-critic architecture for reinforcement learning in the NEST simulator and successfully training it on two different environments from the OpenAI Gym.

1 Introduction

The last decade has witnessed major progress in the field of machine learning, moving from small-scale toy problems to large-scale real-world applications including image [1] and speech recognition [2], complex motor-control tasks [3] and playing (video) games at super-human performance [4, 5]. This progress has been driven mainly by an increase in computing power, especially by training deep networks on graphics processing units [6], and conceptual breakthroughs like layer-wise pretraining [7, 8] or dropout [9]. Even so, this rate of progress would not have been possible without the wide availability of high-performance ready-to-use tools, e.g., Torch [10], Theano [11], Caffe [12], TensorFlow [13] and standardized benchmarks and learning environments, such as the MNIST [14], CIFAR [15] and ImageNET [16] datasets, and the MuJoCo [17], ALE [18] and OpenAI Gym [19] toolkits. While ready-to-use tools allow researchers to focus on important aspects rather than basic implementation details, standardized benchmarks can guide the community as a whole

*These authors contributed equally to this study.

†Corresponding author: j.jordan@fz-juelich.de

towards promising approaches, as for example in the case of convolutional networks through the ImageNET competition [20].

Similarly, researchers in the field of computational neuroscience have benefited from the increase of computational power and achieved many conceptual breakthroughs over the last decade, with a plethora of new neuron, synapse and network models being developed. Thanks to a variety of software projects, researchers have access to simulators for all scales of neural systems from molecular simulations [21] over complex neuron [22, 23] and network models [24–26] to whole brain simulations using neural fields [27]. However, in computational neuroscience no generally accepted set of benchmarks exist so far (but see [28]). While it is desirable to compare different neural network models with respect to biological plausibility, explanatory power and functional performance, only the latter lends itself to the definition of quantitative benchmarks.

One particular area in which the lack of standardized benchmarks is apparent is research into reinforcement learning (RL) in neurobiological substrates. Inspired by behavioural experiments, RL is concerned with the ability of organisms to learn from previous experiences to optimize their behavior in order to maximize reward and avoid punishment (see, e.g., [29]). RL has a long tradition in the field of machine learning which has led to several powerful algorithms, such as SARSA and Q-learning [30]. Similarly, a large variety of neurobiological models have been proposed in recent years [31–44]. However, only a small proportion of these rely on publicly available simulators and all of them employ custom built environments. Even for fairly simple environments, this has led to a situation where different network models are difficult to compare and reproduce, thus creating a fragmentation of research efforts. Instead of building upon and extending existing models, researchers are forced to spend too much time on recreating basic methods for custom implementations.

This issue has led to the Human Brain Project (HBP) [45] dedicating significant resources of a subproject (SP10, Neurorobotics) to the development of the necessary infrastructure that allows users to conduct robotic experiments in virtual environments and connect these to their neural network implementations with an easy to use web interface. This approach however, specifically addresses the need of researchers developing neuronal controllers for robotic applications.

In contrast, the OpenAI Gym [19] provides a rich and generic collection of standardized RL environments developed to support the machine learning community in evaluating and comparing algorithms. All environments are accessible via a simple, unified interface, that requires an agent to supply an action and returns an observation and reward for its current state. The toolkit includes a range of different environments with varying levels of complexity ranging from low-dimensional fully discrete (e.g., *FrozenLake*) to high-dimensional fully continuous tasks (e.g., *Humanoid*). Consistency of the OpenAI Gym environments across different releases supports researchers in reproduction and extension of previous work and allows systematic benchmarking and comparison of learning algorithms and their implementations. The easy accessibility of different tasks fosters progress by allowing researchers to focus on learning algorithms instead of basic implementation details of particular environments and provokes researchers to evaluate the performance of their algorithms on many different tasks.

To make this comprehensive resource available to the computational neuroscience community, we developed a toolchain to interface neural network simulators with the OpenAI Gym. Using this toolchain, researchers can rely on well-tested, high-performance simulation engines to power their models and evaluate them against a curated set of standardized environments, allowing more time to focus on neurobiological questions.

In the next section we introduce additional pre-existing components on which our toolchain relies, and afterwards discuss how it links the different tools. We demonstrate its functionality by implementing a neural actor-critic in NEST ([24], NEural Simulation Tool) and successfully training it on two different environments

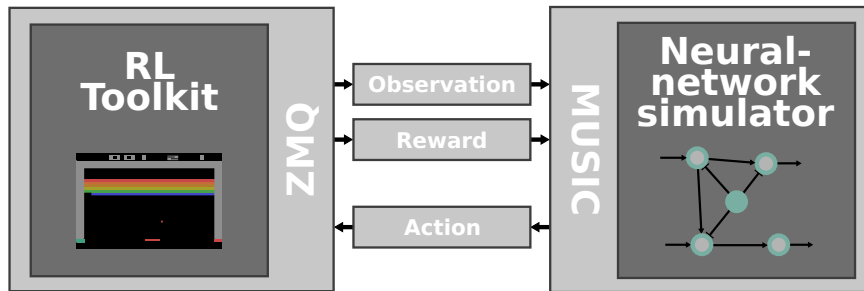


Figure 1: **Interfacing RL toolkits with neural network simulators.** The RL toolkit (left) is responsible for emulating an environment that provides observations and rewards which are communicated via ZeroMQ sockets and MUSIC adapters (middle) to a neural network simulator (right). Concurrently, the activity of the simulated neural network is transformed to an action and fed back to the RL toolkit.

from the OpenAI Gym.

2 Pre-existing components

NEST is a neural simulator designed for the efficient simulation of large-scale networks of simple neuron models with biophysically realistic connectivity. The simulation kernel scales from small simulations on a laptops to super computers, with the largest simulation containing about 10^9 neurons and 10^{13} synapses, corresponding to about 10% of the human cortex at the resolution of individual cells and connections [46]. NEST is actively developed and maintained by the NEST initiative in collaboration with the community and freely available under the GPLv2 and is supported by the HBP with the explicit aim of widespread long-term availability and maintainability.

While the network implementation that we present in the results section relies on the NEST simulator, the toolchain can also be used with other simulators that support the MUSIC library, for example NEURON [22]. The MUlti-Simulation Coordinator is a multi-purpose middleware for neural network simulators built on top of MPI (Message Passing Interface) that enables online interaction of different simulation engines [47]. MUSIC provides named MPI channels, referred to as MUSIC ports, which allow the user to set up communication streams between several processes. While originally intended to distribute a single neural network model across different simulators, the MUSIC library can also be used to connect neural simulators with robotic applications.

For this purpose the ROS-MUSIC Toolchain (RMT) [48] was recently developed, providing an interface from MUSIC to the Robotic Operating System (ROS) [49]. ROS is the most popular middleware in the robotic community which can interact with many robotic simulators and hardware platforms. The RMT allows exchange of well-defined messages between ROS and MUSIC via stand-alone executables, so called adapters, that were designed with a focus on modularity. The toolchain contains several different adapters each performing a rather simple operation on streams of inputs (e.g., filtering). By concatenating several adapters, the overall transformation of the original data can become more complex, for example converting high-dimensional continuous data (e.g., sensory data) to low-dimensional discrete data (e.g., action potentials)

or vice-versa. More information and introductory examples can be found on GitHub.¹

3 Results

To enable the online interaction of neural network simulators and the OpenAI Gym we rely on two different libraries, MUSIC, to interface with the neural simulator, and ZeroMQ [50] to exchange messages with the environment simulated in the OpenAI Gym. In the following we describe these two parts of the toolchain and demonstrate their functionality by interfacing a neural network simulation in NEST with two different environments.

3.1 Extending the ROS - MUSIC toolchain

We extended the RMT by adding adapters that support communication via ZeroMQ following a publish-subscribe pattern. ZeroMQ is a messaging library that allows applications to exchange messages at runtime via sockets. Continuously developed by a large community, it offers bindings for a variety of languages including C++ and Python, and supports most operating systems. A single communication adapter of the RMT sends (receives) data via a ZeroMQ socket and receives (sends) data via a MUSIC port. While the adapters can handle arbitrary data, we defined a set of specialized messages in JSON format (see supplementary material) specifically designed to communicate observations, rewards and actions as discrete or continuous real-valued variables of arbitrary dimensions, as used in the OpenAI Gym. We chose the JSON format due to its simplicity, easy serialization and broad platform support.

In addition to the ZeroMQ adapters dedicated for communication with MUSIC, we developed several further adapters that can perform specific transformations of the data. As discussed above, environments can be defined in continuous or discrete spaces with arbitrary dimensionality. To generate the required closed-loop functionality, the observations provided by the environment must be consistently transformed to a format that can be fed into neural network simulations. Conversely, the activity of the neural network must be interpreted and transformed into valid actions which can be executed in the environment.

A standard way to address the first issue is to introduce so called *place cells*. Each of these cells is tuned to a preferred (multidimensional) observation, i.e., is highly active for a specific input and less active for other inputs [37]. The dependence of the activity of a single place cell on observations is described by its tuning curve, often chosen as a multidimensional Gaussian. To perform the transformation of observations to activity of place cells, we implemented a *discretize adapter* that allows users to specify the position and width of the tuning curves of an arbitrary number of place cells. While having a certain biological plausibility [51], one disadvantage of this approach is that the number of place cells required to cover the whole observation space evenly scales exponentially in the number of dimensions of the observation. For observations with a small number of dimensions, however, this approach is very suitable.

To perform action selection, we added several adapters that can, respectively, select the most active neuron (*argmax adapter*), threshold the activity across neurons to create a binary vector (*threshold adapter*) or linearly combine the activity of neurons across many input channels (*linear decoder*). Depending on the type of action required (discrete/continuous) by the environment, the user can select a single one or a combination of these. See the documentation of the RMT for detailed specifications of the adapters.

In general, we followed the design principle behind the RMT and developed modular adapters. This makes each individual adapter easy to understand and enables users to quickly extend the toolchain with their

¹<https://github.com/incf-music/ros-music-adapters>

own adapters. By combining several adapters, the RMT allows arbitrarily complex transformations of the data and can hence be applied to many use-cases.

3.2 ZeroMQ wrapper for the OpenAI Gym

The second part of the toolchain is a Python wrapper around the OpenAI Gym that exposes ZeroMQ sockets for communicating actions, observations and rewards (see figure 1). An environment in the OpenAI Gym is updated in steps. In each step, an agent needs to provide an action and receives an observation and reward for its current state. The wrapper consists of four different threads that coordinate: (i) performing steps in an environment, (ii) receiving actions via a ZeroMQ SUB socket, (iii) publishing observations via a ZeroMQ PUB socket and (iv) publishing rewards via a ZeroMQ PUB socket. Before spawning the threads, the wrapper starts a user-specified environment and creates the necessary communication buffers. The thread coordinating the environment reads actions from the corresponding buffer, performs single steps in the environment and updates the observation and reward buffers based on the return values of the environment. Upon detecting that a single episode has ended, e.g., by an agent reaching a certain goal position, it resets the environment and allows a user-specified break before starting another episode. The communication threads continuously send(receive) messages via ZeroMQ and read from(write to) the corresponding buffers. All threads can be run with different update intervals, for example, to slow down movement of the agent by performing steps on a coarse time grid whilst continuously receiving action choices from the neural network simulation running on a fine time grid. The user can specify a variety of parameters via a configuration file in JSON format (see supplementary material). See the documentation for detailed specifications of the wrapper.

3.3 Applications

To demonstrate the functionality of the toolchain, we implemented a neural network model with actor-critic architecture in NEST and trained it on two different environments simulated in the OpenAI Gym. In the first task, the agent needs to learn to perform a sequence of actions in order to reach the top of a hill in a continuous environment. The second task is a classical grid-world in which an agent needs to learn to navigate to a goal position in a two-dimensional discrete environment with obstacles. We first describe the neural network architecture and learning rule and afterwards discuss the network’s performance on the two tasks.

3.3.1 Neural network implementation

We consider a temporal-difference learning algorithm [29] implemented as an actor-critic architecture, originally using populations of spiking neurons [37]. We translated the spike-based implementation to rate neurons, mainly to simplify the implementation by avoiding issues arising from noise introduced by spiking neuron models [52, 37]. The neuron dynamics we considered here are determined by the following stochastic differential equation:

$$\tau \frac{dz_i(t)}{dt} = -z_i(t) + \mu_i + f(h_i(t) - \theta_i) + \xi_i(t), \quad (1)$$

where τ is some positive time constant, μ_i a baseline activity level, $f(\cdot)$ some (arbitrary) activation function, $h_i(t)$ a time dependent input field, θ_i an input threshold and $\xi_i(t)$ white noise with a certain standard deviation σ_ξ . The input field $h_i(t)$ is determined by the activity of other neurons according to $h_i(t) = \sum_j w_{ij} z_j(t)$, with w_{ij} denoting the strength of the connection (weight) from neuron j to neuron i . Here we will exclusively consider activation functions of the form $f(x) = x$ (linear case), and $f(x) = \Theta(x)x$ (threshold-linear case,

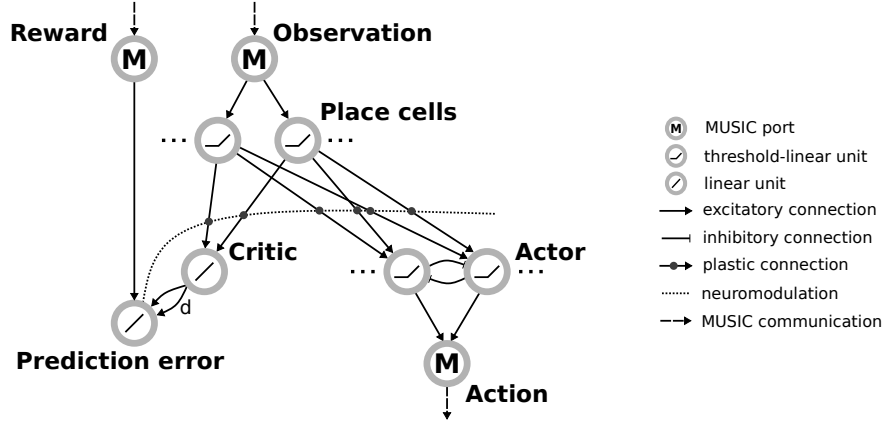


Figure 2: **Actor-critic architecture for RL with rate neurons.** Observations are communicated via a MUSIC input port to a population of place cells. These project on the one hand to a critic unit and on the other hand to actor units arranged in a winner-take-all circuit. The critic and an additional MUSIC input port project to a unit representing the reward-prediction error that modulates the plasticity between place cells and critic and actors, respectively. The actor units project to a MUSIC output port encoding the selected action.

“relu”). These models have recently been added to the NEST simulator. Their dynamics are solved on a fixed time-grid by a stochastic-exponential-Euler method with a step size determined by the resolution of the simulation. For more details on the model implementation see [53].

The input layer is a population of threshold-linear rate neurons which receive inputs through MUSIC and encode observations from the environment (see figure 2). Via plastic connections these place cells project to a single neuron representing the value that the network assigns to the current state (the “critic”). An additional neuron calculates the reward-prediction error by combining the reward received from the environment with input from the critic. Plasticity of the projections from inputs to the critic is modulated by this reward-prediction error (see below).

In addition, neurons in the input layer project to a population of neurons representing the available actions (the “actor”). To enforce selection of a specific action, the actor units are arranged in a winner-take-all (WTA) circuit. This is implemented by recurrent connections between actor units that correspond to short-range excitation and long-range inhibition, depending on the similarity of the action that actor units encode. The activity of actor units is transformed to a valid action and communicated to the environment via the RMT.

To derive a learning rule for the critic, we followed similar steps as in [37] applied to rate models (equation (1)). The critic activity should approximate a continuous-time value function defined by [54]

$$V^\pi(\mathbf{s}(t)) := \int_{t'}^{\infty} r(\mathbf{s}^\pi(t')) e^{-\frac{t'-t}{\tau_r}} dt'. \quad (2)$$

Here $\mathbf{s}(t)$ denotes the state of the agent at time t , $r(\mathbf{s}^\pi(t))$ denotes the reward obtained in state $\mathbf{s}(t)$, τ_r a discounting factor for future rewards and π the agent’s policy. To achieve this, we define the following objective function which should be minimized by gradient descent on the weights from inputs to the critic:

$$E(t) = \frac{1}{2} (V^\pi(t) - z(t))^2, \quad (3)$$

where $z(t)$ represents the activity of the critic unit. By performing gradient descent on equation (3), using a self-consistency equation for $V^\pi(t)$ from the derivative of equation (2) and bootstrapping on the current prediction for the value (see supplementary material and [54, 37]), we obtain the following local Hebbian three-factor learning rule that approximately minimizes the objective function (equation (3)):

$$\Delta w_j = \eta \delta(t) x_j(t) \Theta(z(t) - \theta_{\text{post}}) , \quad (4)$$

where η is a learning rate, $x_j(t)$ represents the activity of the j th place cell, $\Theta(\cdot)$ the Heaviside function and θ_{post} a parameter that accounts for noise on the postsynaptic unit (see supplementary material for details). The term $\delta(t) = \dot{v}(t) + r(t) - \frac{1}{\tau_r} v(t)$ corresponds to the activity of the reward-prediction error unit, acting as a neuromodulatory signal for the Hebbian plasticity between the presynaptic (x_j) and postsynaptic (z) units. To avoid explicit calculation of the derivative, we rewrite $\delta(t)$ as:

$$\delta(t) \approx \left(\frac{1}{d} - \frac{1}{\tau_r} \right) v(t) - \frac{1}{d} v(t-d) + r(t) . \quad (5)$$

To approximate the derivative we hence implement two connections from the critic to the reward-prediction error unit: one instantaneous, and one with delay $d > 0$.

To learn an optimal policy, we exploit that the actor units follow the same dynamics as the critic. Similar to [37], we hence apply the same learning rule to the connections between the inputs and the actor units. In order to assure that at least one actor unit is active, thus preventing a deadlock, we introduce a minimal weight for each connection between input and output units and add input noise to the actor units.

3.3.2 Mountain Car

As an example of an environment with continuous states, we consider the *MountainCar* environment. The task is to steer a toy vehicle that starts at a valley between two hills to the top of the right one (figure 3A, inset). To make the task more challenging, the car’s engine is not strong enough to reach the top in one go, so the agent needs to learn to gain momentum by swinging back and forth between the two hills. A single episode in this environment starts when the agent is placed in the valley and ends when it reaches the final position on the top of the right hill. The state of the agent is described by two continuous variables: the x-position $x(t)$ and the x-velocity $\dot{x}(t)$. The agent can choose from three different discrete actions that affect the velocity of the vehicle (accelerate left, no acceleration, accelerate right). It receives punishment from the environment in every step; the goal is to minimize the total punishment collected over the whole episode. Since this is difficult to implement in an actor-critic architecture [52], we provide additional reward when the agent reaches the final position.

To translate the agent’s current state into neuronal activity, we distribute 25 place cells evenly across the two dimensional plane of possible positions and velocities using the *discretize adapter* of the RMT. The actor is implemented by a WTA circuit of three units as described in section 3.3.1. The activity of these units is transformed into an action via the *argmax adapter* (section 3.1).

Initially, the agent explores the environment by selecting random actions. Due to the WTA circuit dynamics, a single action stays active over an extended period of time. The constant punishment gradually decreases the weights from the place cells to the corresponding actor unit, eventually leading to another actor unit becoming active (figure 3B, left). After a while, the agent reaches the goal by performing actions that have not been significantly punished. For this task the stable nature of the WTA is advantageous, causing the agent to perform the same action repeatedly allowing efficient exploration of the state space. After the agent has found the goal once, the number of steps spent on exploring actions in the following episodes is much smaller. From the sixth episode on, the performance of the agent is already close to optimal (figure 3A).

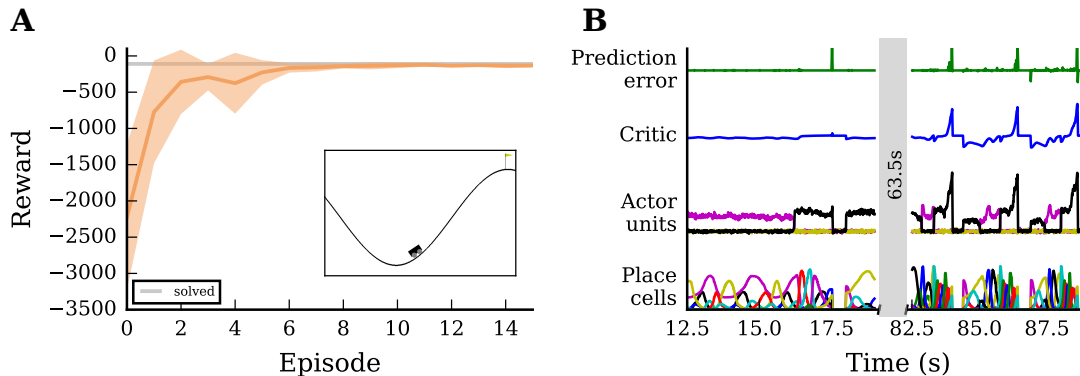


Figure 3: **Network performance on an environment with continuous states and discrete actions.** **A:** Reward obtained by the agent per episode averaged over 10 simulations with different seeds (solid orange line). Orange band indicates \pm one standard deviation. Light gray line marks average reward per episode for which the environment is considered solved. Inset: screenshot of the environment with agent (stylized vehicle), environment with valley and two hills (black solid line) and goal position (yellow flag). The agent is close to the starting position at the trough. **B:** Activity traces of place cells (bottom), actor units (second from bottom), critic unit (second from top) and reward-prediction-error unit (top). Shown are neural activities during 6.5 s early (left) and late (right) in the simulation.

After learning for about 10 episodes, the agent’s performance has converged. The value of the final state is successfully propagated backwards over different states, leading to a ramping of activity of the critic unit from the start of an episode to the end (figure 3B, right).

Since the OpenAI Gym offers a variety of environments, we trained the same network model on an additional task with different requirements.

3.3.3 Frozen Lake

As a second application, we chose the *FrozenLake* environment consisting of a discrete set of 16 states arranged in a four-by-four grid (figure 4A, inset). Each state is either a start state (S), a goal state (G), a hole (H) or a frozen state (F). From the start position, the agent has to reach the rewarded state by navigating over the frozen states without falling into holes which would reset the agent to the starting position. In each step, the agent can choose from four different actions: move west, move north, move east and move south. Usually, the tiles are “slippery”, i.e., there is a chance that a random action is executed irrespective of the action chosen by the agent. However, to simplify learning for demonstration purposes, we turned this feature off. Upon reaching the goal, the agent receives a reward of magnitude one. Since the optimal path involves six steps from start to goal, the theoretical optimal reward per step is ~ 0.16 . To encourage exploration, the agent receives a small punishment in each state, and additionally, to speed up learning, the agent is punished for falling into holes.

Unlike in the continuous *MountainCar* environment, the tuning curves of place cells do not overlap in the discrete case, leading to sharp transitions in the network activity. This leads to severe issues for associating values and actions with the respective states. To address this problem we introduced a simple eligibility trace by evaluating the activity of the pre- and post synaptic units in the learning rule with a small delay δt (see supplementary material). With this addition, the network model is able to find the optimal solution for this

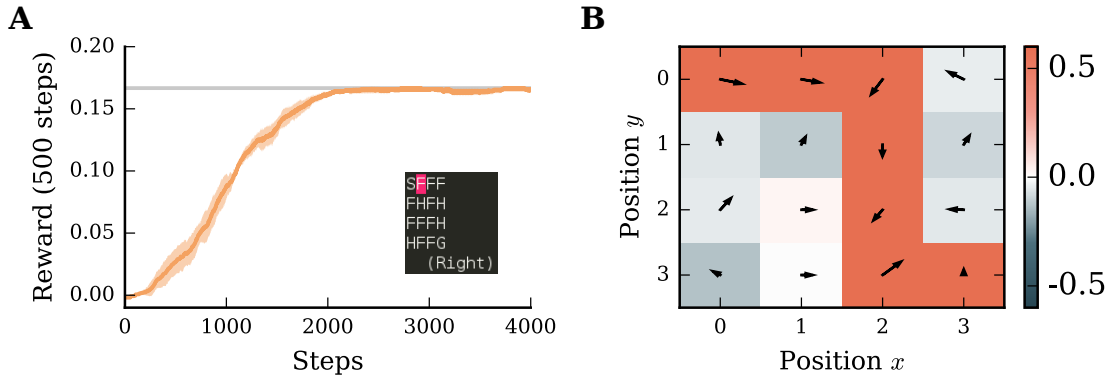


Figure 4: **Network performance on a grid-world environment.** **A:** Average reward collected by the agent over the next 500 steps (orange solid line) averaged over 5 simulations. Orange band indicates \pm one standard deviation. Gray line: theoretical optimum. Inset: screenshot of the environment with start state (S), frozen states (F), holes (H) and goal state (G). The position of the agent is indicated in pink. **B:** The learned policy and value map of the environment. Red colors indicate positive, blue colors negative values. Arrows indicate the preferred direction of movement.

task within roughly 2000 steps (figure 4A). It also learns to associate holes with punishment and frozen states with reward if they are on the path to the goal (figure 4B). Although there are two possible paths to the goal, the agent prefers the path with less corners, since it is easier to navigate using a WTA circuit.

4 Conclusion

In this manuscript, we have presented a toolchain that closes the loop between the OpenAI Gym and neural network simulators. We demonstrated the functionality of the toolchain by implementing an actor-critic architecture in NEST and evaluating its performance on two different environments. The performance of the network quickly reached near-optimal performance on these two tasks.

Combining neural network simulators with RL toolkits responds to the growing need of researchers to provide neural network models with rich, dynamic input. Compared to creating customized environments to this end, using readily available tools is easier, often computationally more efficient, and most importantly, supports reproducible science. In addition, having the OpenAI Gym environments as common benchmarks in both fields encourages comparison between traditional machine learning and biologically plausible implementations. In contrast to models presented in previous studies, our toolchain makes it easy for other researchers to extend our implementation of an actor-critic architecture to other environments, replace neurons models or explore alternative learning rules.

While the toolchain currently only supports the OpenAI Gym, the extension to other toolkits is simple due to a modular design of the wrapper. The RMT can be found on GitHub and is available under the GPLv3. The OpenAI Gym ZeroMQ wrapper is also available via GitHub under the MIT license. A complementary development to the work presented here is provided by SPORE, a framework for reward-based learning with spiking neurons in the NEST simulator.² It provides support for synapse models with time-driven updates,

²<https://github.com/IGITUGraz/spore-nest-module>

additional support for recording and evaluating traces of neuronal state variables and introduces MUSIC ports for communicating rewards to a running simulation.

With the work presented here we enable researchers to build more easily upon previous studies and evaluate novel models. We hope this boosts the progress in computational neuroscience in uncovering the biophysical mechanisms involved in learning complex tasks from delayed rewards.

Acknowledgments

We acknowledge partial support by the German Federal Ministry of Education through our German-Japanese Computational Neuroscience Project (BMBF Grant 01GQ1343), EuroSPIN, the Helmholtz Alliance through the Initiative and Networking Fund of the Helmholtz Association and the Helmholtz Portfolio theme “Supercomputing and Modeling for the Human Brain” and the European Union Seventh Framework Programme (FP7/2007-2013) under grant agreement no. 604102 (HBP). All network simulations carried out with NEST (<http://www.nest-simulator.org>).

References

- [1] Krizhevsky, A., Sutskever, I., & Hinton, G. E. (2012). Imagenet classification with deep convolutional neural networks. In *Advances in neural information processing systems*, pp. 1097–1105.
- [2] Hinton, G., Deng, L., Yu, D., Dahl, G. E., Mohamed, A.-r., Jaitly, N., Senior, A., Vanhoucke, V., Nguyen, P., Sainath, T. N., et al. (2012a). Deep neural networks for acoustic modeling in speech recognition: The shared views of four research groups. *IEEE Signal Processing Magazine* 29(6), 82–97.
- [3] Mnih, V., Badia, A. P., Mirza, M., Graves, A., Lillicrap, T., Harley, T., Silver, D., & Kavukcuoglu, K. (2016). Asynchronous methods for deep reinforcement learning. In *International Conference on Machine Learning*, pp. 1928–1937.
- [4] Mnih, V., Kavukcuoglu, K., Silver, D., Rusu, A. A., Veness, J., Bellemare, M. G., Graves, A., Riedmiller, M., Fidjeland, A. K., Ostrovski, G., et al. (2015). Human-level control through deep reinforcement learning. *Nature* 518(7540), 529–533.
- [5] Silver, D., Huang, A., Maddison, C. J., Guez, A., Sifre, L., Van Den Driessche, G., Schrittwieser, J., Antonoglou, I., Panneershelvam, V., Lanctot, M., et al. (2016). Mastering the game of go with deep neural networks and tree search. *Nature* 529(7587), 484–489.
- [6] Raina, R., Madhavan, A., & Ng, A. Y. (2009). Large-scale deep unsupervised learning using graphics processors. In *Proceedings of the 26th annual international conference on machine learning*, pp. 873–880. ACM.
- [7] Hinton, G. E., & Salakhutdinov, R. R. (2006). Reducing the dimensionality of data with neural networks. *Science* 313(5786), 504–507.
- [8] Bengio, Y., Lamblin, P., Popovici, D., Larochelle, H., et al. (2007). Greedy layer-wise training of deep networks. *Advances in neural information processing systems* 19, 153.
- [9] Hinton, G. E., Srivastava, N., Krizhevsky, A., Sutskever, I., & Salakhutdinov, R. R. (2012b). Improving neural networks by preventing co-adaptation of feature detectors. *arXiv preprint arXiv:1207.0580*.
- [10] Collobert, R., Bengio, S., & Mariéthoz, J. (2002). Torch: a modular machine learning software library. Technical report, Idiap.

- [11] James, B., Olivier, B., Frédéric, B., Pascal, L., & Razvan, P. (2010). Theano: a cpu and gpu math expression compiler. In *Proceedings of the Python for Scientific Computing Conference (SciPy)*.
- [12] Jia, Y., Shelhamer, E., Donahue, J., Karayev, S., Long, J., Girshick, R., Guadarrama, S., & Darrell, T. (2014). Caffe: Convolutional architecture for fast feature embedding. *arXiv preprint arXiv:1408.5093*.
- [13] Abadi, M., Agarwal, A., Barham, P., Brevdo, E., Chen, Z., Citro, C., Corrado, G. S., Davis, A., Dean, J., Devin, M., et al. (2016). Tensorflow: Large-scale machine learning on heterogeneous distributed systems. *arXiv preprint arXiv:1603.04467*.
- [14] LeCun, Y., Cortes, C., & Burges, C. J. (1998). The mnist database of handwritten digits.
- [15] Krizhevsky, A., & Hinton, G. (2009). Learning multiple layers of features from tiny images.
- [16] Deng, J., Dong, W., Socher, R., Li, L.-J., Li, K., & Fei-Fei, L. (2009). ImageNet: A Large-Scale Hierarchical Image Database. In *CVPR09*.
- [17] Todorov, E., Erez, T., & Tassa, Y. (2012). Mujoco: A physics engine for model-based control. In *Intelligent Robots and Systems (IROS), 2012 IEEE/RSJ International Conference on*, pp. 5026–5033. IEEE.
- [18] Bellemare, M., Naddaf, Y., Veness, J., & Bowling, M. (2015). The arcade learning environment: An evaluation platform for general agents. In *Twenty-Fourth International Joint Conference on Artificial Intelligence*.
- [19] Brockman, G., Cheung, V., Pettersson, L., Schneider, J., Schulman, J., Tang, J., & Zaremba, W. (2016). OpenAI Gym. *ArXiv e-prints*.
- [20] Russakovsky, O., Deng, J., Su, H., Krause, J., Satheesh, S., Ma, S., Huang, Z., Karpathy, A., Khosla, A., Bernstein, M., Berg, A. C., & Fei-Fei, L. (2015). ImageNet Large Scale Visual Recognition Challenge. *International Journal of Computer Vision (IJCV) 115*(3), 211–252.
- [21] Wils, S., & De Schutter, E. (2009). STEPS: modeling and simulating complex reaction-diffusion systems with Python. *Front. Neuroinformatics 3*(15).
- [22] Carnevale, T., & Hines, M. (2006). *The NEURON Book*. Cambridge: Cambridge University Press.
- [23] Bower, J. M., & Beeman, D. (2007). GENESIS (simulation environment). *Scholarpedia 2*(3), 1383.
- [24] Gewaltig, M.-O., & Diesmann, M. (2007). NEST (NEural Simulation Tool). *Scholarpedia 2*(4), 1430.
- [25] Goodman, D. F. M., & Brette, R. (2009). The Brian simulator. *Front. Neurosci. 3*(2), 192–197. doi: 10.3389/neuro.01.026.2009.
- [26] Bekolay, T., Bergstra, J., Hunsberger, E., DeWolf, T., Stewart, T. C., Rasmussen, D., Choo, X., Voelker, A. R., & Eliasmith, C. (2013). Nengo: a python tool for building large-scale functional brain models. *Frontiers in neuroinformatics 7*.
- [27] Sanz Leon, P., Knock, S., Woodman, M., Domide, L., Mersmann, J., McIntosh, A., & Jirsa, V. (2013). The virtual brain: a simulator of primate brain network dynamics. *Front. Neuroinform. 7*, 10.
- [28] Gerstner, W., & Naud, R. (2009). How good are neuron models? *Science 326*(5951), 379–380.
- [29] Sutton, R. S., & Barto, A. G. (1998). *Reinforcement Learning: An Introduction*. Adaptive Computation and Machine Learning. The MIT Press.
- [30] Watkins, C. J. C. H. (1989). *Learning from delayed rewards*. Ph. D. thesis, University of Cambridge England.

- [31] Vasilaki, E., Frémaux, N., Urbanczik, R., Senn, W., & Gerstner, W. (2009). Spike-based reinforcement learning in continuous state and action space: When policy gradient methods fail. *PLoS Comput. Biol.* 5(12), e1000586. doi:10.1371/journal.pcbi.1000586.
- [32] Izhikevich, E. M. (2007). Solving the distal reward problem through linkage of STDP and dopamine signaling. *Cereb. Cortex* 17(10), 2443–2452.
- [33] Urbanczik, R., & Senn, W. (2009). Reinforcement learning in populations of spiking neurons. *Nature neuroscience* 12(3), 250.
- [34] Potjans, W., Morrison, A., & Diesmann, M. (2009). A spiking neural network model of an actor-critic learning agent. *Neural Comput.* 21, 301–339.
- [35] Frémaux, N., Sprekeler, H., & Gerstner, W. (2010). Functional requirements for reward-modulated spike-timing-dependent plasticity. *J. Neurosci.* 30(40), 13326–13337.
- [36] Jitsev, J., Morrison, A., & Tittgemeyer, M. (2012). Learning from positive and negative rewards in a spiking neural network model of basal ganglia. In *Neural Networks (IJCNN), The 2012 International Joint Conference on*, pp. 1–8. IEEE.
- [37] Frémaux, N., Sprekeler, H., & Gerstner, W. (2013). Reinforcement learning using a continuous time actor-critic framework with spiking neurons. *PLoS Comput Biol* 9(4), e1003024.
- [38] Rasmussen, D., & Eliasmith, C. (2014). A neural model of hierarchical reinforcement learning. In *CogSci*.
- [39] Friedrich, J., Urbanczik, R., & Senn, W. (2014). Code-specific learning rules improve action selection by populations of spiking neurons. *International Journal of Neural Systems* 24(05), 1450002.
- [40] Rombouts, J. O., Bohte, S. M., & Roelfsema, P. R. (2015). How attention can create synaptic tags for the learning of working memories in sequential tasks. *PLoS Comput Biol* 11(3), e1004060.
- [41] Baladron, J., & Hamker, F. H. (2015). A spiking neural network based on the basal ganglia functional anatomy. *Neural Networks* 67, 1–13.
- [42] Aswolinskiy, W., & Pipa, G. (2015). Rm-sorn: a reward-modulated self-organizing recurrent neural network. *Frontiers in computational neuroscience* 9, 36.
- [43] Friedrich, J., & Lengyel, M. (2016). Goal-directed decision making with spiking neurons. *Journal of Neuroscience* 36(5), 1529–1546.
- [44] Rueckert, E., Kappel, D., Tanneberg, D., Pecevski, D., & Peters, J. (2016). Recurrent spiking networks solve planning tasks. *Scientific reports* 6.
- [45] Human Brain Project (2014). Project website. Available at: <http://www.humanbrainproject.eu>.
- [46] Kunkel, S., Schmidt, M., Eppler, J. M., Masumoto, G., Igarashi, J., Ishii, S., Fukai, T., Morrison, A., Diesmann, M., & Helias, M. (2014). Spiking network simulation code for petascale computers. *Front. Neuroinformatics* 8, 78.
- [47] Djurfeldt, M., Hjorth, J., Eppler, J. M., Dudani, N., Helias, M., Potjans, T. C., Bhalla, U. S., Diesmann, M., Kotaleski, J. H., & Ekeberg, O. (2010). Run-time interoperability between neuronal simulators based on the music framework. *Neuroinformatics* 8. doi:10.1007/s12021-010-9064-z.
- [48] Weidel, P., Djurfeldt, M., Duarte, R. C., & Morrison, A. (2016). Closed loop interactions between spiking neural network and robotic simulators based on music and ros. *Frontiers in neuroinformatics* 10.

- [49] Quigley, M., Conley, K., Gerkey, B., Faust, J., Foote, T., Leibs, J., Wheeler, R., & Ng, A. Y. (2009). Ros: an open-source robot operating system. In *ICRA workshop on open source software*, Volume 3, pp. 5. Kobe.
- [50] Hintjens, P. (2013). *ZeroMQ: Messaging for Many Applications*. "O'Reilly Media, Inc."
- [51] Moser, E. I., Kropff, E., & Moser, M.-B. (2008). Place cells, grid cells, and the brain's spatial representation system. *Annu. Rev. Neurosci.* 31, 69–89.
- [52] Potjans, W., Diesmann, M., & Morrison, A. (2011). An imperfect dopaminergic error signal can drive temporal-difference learning. *PLoS Comput. Biol.* 7(5), e1001133.
- [53] Hahne, J., Dahmen, D., Schuecker, J., Frommer, A., Bolten, M., Helias, M., & Diesmann, M. (2016). Integration of continuous-time dynamics in a spiking neural network simulator. *arXiv*. 1610.09990 [q-bio.NC].
- [54] Doya, K. (2000). Reinforcement learning in continuous time and space. *Neural Comput.* 12(1), 219–245.
- [55] Nordlie, E., Gewaltig, M.-O., & Plesser, H. E. (2009). Towards reproducible descriptions of neuronal network models. *PLoS Comput. Biol.* 5(8), e1000456.

Supplementary material

A Derivation of the learning rule

We consider continuous time, continuous states and continuous actions and follow similar steps as [54, 37]. Starting from the continuous-time value function

$$V^\pi(\mathbf{s}(t)) := \int_t^\infty r(\mathbf{s}^\pi(t')) e^{-\frac{t'-t}{\tau_r}} dt', \quad (6)$$

we take the derivative with respect to t to arrive at a self-consistency equation for V :

$$\dot{V}^\pi(t) := \frac{dV^\pi(t)}{dt} = -r(t) + \frac{1}{\tau_r} V^\pi(t). \quad (7)$$

To implement temporal-difference learning in a neural network architecture, we would like to approximately represent the true value $V^\pi(t)$ of the state at time t by the rate $z_i(t)$ of a critic neuron. This activity will depend on the activity of input units, i.e., place cells, and the weights between inputs and critic. With initially random weights the self-consistency criterion will not be fulfilled, and will have a finite error $\delta(t)$:

$$\delta(t) = \dot{z}_i(t) + r(t) - \frac{1}{\tau_r} z_i(t). \quad (8)$$

We now define an objective function that should be minimized by gradient descent on the weights:

$$E(t) = \frac{1}{2} (V^\pi(t) - z_i(t))^2. \quad (9)$$

We take derivative with respect to w_{ij} and use the self-consistency equation (7):

$$\begin{aligned} \frac{\partial E(t)}{\partial w_{ij}} &= -(V^\pi(t) - z_i(t)) \frac{\partial z_i(t)}{\partial w_{ij}} \\ &= -(\tau_r \dot{V}^\pi(t) + \tau_r r(t) - z_i(t)) \frac{\partial z_i(t)}{\partial w_{ij}} \\ &\approx -\underbrace{(\tau_r \dot{z}_i(t) + \tau_r r(t) - z_i(t))}_{\tau_r \delta(t)} \frac{\partial z_i(t)}{\partial w_{ij}} \end{aligned} \quad (10)$$

Here we have replaced $\dot{V}^\pi(t)$ with $\dot{z}_i(t)$ in the last line. For a discussion of the validity of this approximation and the convergence of the learning rule, see [37]. To perform gradient descent on the objective function, we hence need to change the weights according to

$$\begin{aligned}\Delta w_{ij} &:= -\eta' \frac{\partial E(t)}{\partial w_{ij}} \\ &= \eta \delta(t) \frac{\partial z_i(t)}{\partial w_{ij}},\end{aligned}\tag{11}$$

where we introduced $\eta = \eta' \tau_r$. We hence need to determine the derivative of the critic activity with respect to the weights between inputs and critic $\frac{\partial z_i(t)}{\partial w_{ij}}$.

We start from the differential equation describing the dynamics of a threshold-linear rate neuron, and assume the noise to be small, i.e., we drop the term $\xi_i(t)$. Without loss of generality, we assume $\mu_i = 0, \theta_i = 0$. The dynamics are then given by the solution to

$$\tau \frac{dz_i(t)}{dt} = -z_i(t) + g \Theta \left(\sum_j w_{ij} x_j(t) \right) \left(\sum_j w_{ij} x_j(t) \right).\tag{12}$$

Variation of constants yields the general solution as a convolution equation:

$$z_i(t) = g \left(\left(\Theta(\dots) \left(\sum_j w_{ij} x_j(\cdot) \right) \right) * \kappa(\cdot) \right) (t),\tag{13}$$

where we have introduced the filter kernel $\kappa(t) = \frac{1}{\tau} e^{-\frac{t}{\tau}} \Theta(t)$. We now take the derivative with respect to w_{ij} . While the derivative at $\sum_j w_{ij} x_j(t) = 0$ is technically not defined, we follow the usual convention and set it to zero. This yields

$$\frac{\partial z_i(t)}{\partial w_{ij}} = \begin{cases} g(x_j * \kappa)(t) & \text{if } \sum_j w_{ij} x_j(t) > 0 \\ 0 & \text{else} \end{cases}\tag{14}$$

By combining equation (11) with equation (14), we obtain the following learning rule:

$$\Delta w_{ij} = \begin{cases} \eta \delta(t) g(x_j * \kappa)(t) & \text{if } \sum_j w_{ij} x_j(t) > 0 \\ 0 & \text{else} \end{cases}\tag{15}$$

By choosing the time constant of critic and actors small, we effectively remove the filtering of the presynaptic activity ($\lim_{\tau \rightarrow 0} \kappa(t) = \delta(t)$) and hence ignore it. To simplify this equation further, we rewrite it as a condition on the rate of the postsynaptic neuron by observing that $z_i(t) > 0$ iff $\sum_j w_{ij} x_j(t) > 0$. To implement exploration for similar inputs to all output units we add noise to the activity of the actor units. We only consider a postsynaptic neuron active, if its activity is larger than some threshold θ_{post} . This leads to the following form for the learning rule:

$$\Delta w_{ij} = \eta \delta(t) g x_j(t) \Theta(z_i(t) - \theta_{\text{post}}),\tag{16}$$

where we $\Theta(\cdot)$ denotes the Heaviside step function defined as:

$$\Theta(x) = \begin{cases} 1 & x > 0 \\ 0 & \text{else} \end{cases}$$

To implement a simple type of eligibility trace, we introduce an additional parameter δt that can delay the activity of the pre- and post-synaptic units in the learning rule:

$$\Delta w_{ij} = \eta \delta(t) g x_j(t - \delta t) \Theta(z_i(t - \delta t) - \theta_{\text{post}}),\tag{17}$$

A		Model summary	
Populations	Seven		
Topology	None		
Connectivity	Population specific		
Neuron model	Linear & threshold-linear rate		
Channel models	None		
Synapse model	Instantaneous & delayed continuous coupling		
Plasticity	Three-factor Hebbian		
External input	Continuous MUSIC ports		
External output	Continuous MUSIC ports		
Measurements	Rates of all neurons		
B		Populations	
Name	Elements	Size	
Observation	MUSIC in port	1	
Reward	MUSIC in port	1	
Action	MUSIC out port	1	
Place cells	Threshold-linear	16(25)	
Critic	Threshold-linear	1	
Actor	Threshold-linear	4(3)	
Prediction error	Linear	1	
C		Connectivity	
Source	Target	Pattern	
Observation	Place cells	One-to-one (by MUSIC channel), instantaneous, static, weight w_o	
Reward	Prediction error	One-to-one (by MUSIC channel), instantaneous, static, weight w_r	
Actor	Action	One-to-one (by MUSIC channel), instantaneous, static, weight w_a	
Place cells	Critic	All-to-all, instantaneous, plastic, initial weight w_{pc}	
Place cells	Actor	All-to-all, instantaneous, plastic, initial weight w_{pa}	
Critic	Prediction error	One-to-one, instantaneous, static, weight $1/d - 1/\tau_r$	
Critic	Prediction error	One-to-one, delay d , static, weight $-1/d$	
Actor	Actor	All-to-all, instantaneous, static, weight $\alpha \exp(-\Delta a/\sigma) + \beta$	
D		Neuron and synapse model	
Type	Linear rate neuron		
Dynamics	$\tau \frac{dz(t)}{dt} = -z(t) + \mu + (h(t) - \theta) + \xi(t)$		
Type	Threshold-linear rate neuron		
Dynamics	$\tau \frac{dz(t)}{dt} = -z(t) + \mu + \Theta(h(t) - \theta)(h(t) - \theta) + \xi(t)$		
Type	Three-factor Hebbian synapse		
Plasticity	$\Delta w_{ij} = \eta \delta(t) g x_j(t - \delta t) \Theta(z_i(t - \delta t) - \theta_{post})$		
E		Input	
Type	Description		
Observation	Rate $r \in [-1, 1]$ according to tuning of place cell (using <i>discretize</i> adapter)		
Reward	Rate $r \in [-1, 1]$ according to reward provided by the environment		
F		Output	
Type	Description		
Action	Rates $r_i \in [0, \infty)$ according to activities of the actor units		

Table 1: Description of the network model (according to [55]).

B		Populations: place cells	
Name	Values		
τ	5.0 (1.0)		
g	1.0		
μ	0.0		
σ_ξ	0.0		
θ	-0.5		
B		Populations: critic	
Name	Values		
τ	0.1		
g	1.0		
μ	-1.0		
σ_ξ	0.0		
θ	-1.0		
B		Populations: reward	
Name	Values		
τ	1.0		
g	1.0		
μ	0.0		
σ_ξ	0.0		
θ	0.001 (-0.0999)		
B		Populations: actor	
Name	Values		
τ	0.1		
g	1.0		
μ	0.0		
σ_ξ	0.2 (0.05)		
θ	0.0		
C		Connectivity	
Name	Values		
w_o	0.5		
w_r	0.1		
w_a	1.0		
w_{pc}	0.0		
w_{pc}^{\min}	-1.0		
w_{pc}^{\max}	1.0		
θ_{post}^{pc}	-1.0		
w_{pa}	0.9(0.3)		
w_{pa}^{\min}	0.1(0.05)		
w_{pa}^{\max}	1.0		
θ_{post}^{pa}	0.5(0.1)		
d	1.0		
τ_r	20000.0		
α	1.2		
β	-0.55		
σ_ξ	0.1		
η_{critic}	0.01(0.125)	16	
η_{actor}	0.2(0.250)		
δt	19.0(0.0)		
E		Input: discretize adapter	
Name	Values		
σ_x	0.01 (0.2)		
σ_y	- (0.2)		

Table 2: Table of the network parameters used for both tasks (according to [55]). Values in brackets are used for the *MountainCar* environment

B Network description

The tables 1 and 2 summarize the network architecture and parameters.

C JSON Message types

Listing 1 show the standard message types used for communication between the OpenAI Gym and the RMT. All messages are serialized using JSON and communicated via ZeroMQ.

Listing 1: Message types used for communication.

```
BasicMsg
{
    float min
    float max
    float value
    float timestamp
}

ObservationMsg
{
    BasicMsg[] observations    # one basic msg per dimension
}

RewardMsg
{
    BasicMsg[] reward         # reward is always one dimensional
}

ActionMsg
{
    BasicMsg[] actions        # one dimensional for discrete actions
                              # or one dimension per possible action
}
```

D Example wrapper configuration file

Listing 2 shows an example configuration file for running the mountain car environment.

Listing 2: Example configuration file for the wrapper to run the “MountainCar-v0” environment.

```
"All":
{
    "seed": 12345,
    "time_stamp_tolerance": 0.01,
    "prefix": null,
    "write_report": true,
    "report_file": "./report.json",
    "overwrite_files": false,
    "flush_report_interval": null
}
```

```

    },
    "Env":
    {
        "env": "MountainCar-v0",
        "initial_reward": null,
        "final_reward": null,
        "min_reward": -1.0,
        "max_reward": 1.0,
        "render": true,
        "monitor": false,
        "monitor_dir": "./experiment-0/",
        "monitor_args":
        {
            "write_upon_reset": true,
            "video_callable": false
        }
    },
    "EnvRunner":
    {
        "update_interval": 0.01,
        "inter_trial_duration": 0.4
    },
    "CommandReceiver":
    {
        "socket": 5555,
        "time_stamp_tolerance": 0.01
    },
    "ObservationSender":
    {
        "socket": 5556,
        "update_interval": 0.01
    },
    "RewardSender":
    {
        "socket": 5557,
        "update_interval": 0.01
    }
}

```

E Example MUSIC configuration file

Listing 3 shows an example MUSIC configuration file to run the MountainCar environment. It shows the different processes with parameters which are spawned by MUSIC including RMT adapters and NEST.

Listing 3: Example MUSIC configuration file to run the MountainCar environment.

```

stoptime=150.
rtf=1.
[reward]
binary=zmq_in_adapter
args=

```

```

np=1
music_timestep=0.001
message_type=GymObservation
zmq_topic=
zmq_addr=tcp://localhost:5557
[ sensor ]
binary=zmq_in_adapter
args=
np=1
music_timestep=0.001
message_type=GymObservation
zmq_topic=
zmq_addr=tcp://localhost:5556
[ discretize ]
binary=discretize_adapter
args=
np=1
music_timestep=0.001
grid_positions_filename=grid_pos.json
[ nest ]
binary=./actor_critic_network/network.py
args=-t 150. -n 25 -m 3 -p network_params.json
np=1
[ argmax ]
binary=argmax_adapter
args=
np=1
music_timestep=0.001
[ command ]
binary=zmq_out_adapter
args=
np=1
music_timestep=0.01
message_type=GymCommand
zmq_topic=
zmq_addr=tcp://*:5555
sensor.out->discretize.in[2]
discretize.out->nest.in[25]
reward.out->nest.reward_in[1]
nest.out->argmax.in[3]
argmax.out->command.in[1]

```

F Environments

Table F shows parameters for the OpenAI Gym environments and the ZeroMQ wrapper.

OpenAI Gym	
Name	Values
Version	0.8.1
MountainCar	
Name	Values
Version	0
Max episode steps	None
Initial reward*	-1.0
Final reward*	-0.4
Inter-trial duration*	0.4
Update interval (env runner)*	0.02
FrozenLake	
Name	Values
Version	0
Max episode steps	None
Slippery	False
Final reward null*	-0.1
Inter-trial duration*	0.1
Update interval (env runner)*	0.1

Table 3: Table of the environment parameters. Values marked with * indicate values for the ZeroMQ wrapper.